Optimizing Dye-Sensitized Solar Cell (DSSC) Performance through Synergistic Natural Dye Combinations from *Beta vulgaris* L., *Curcuma longa* L., and *Pandanus amaryllifolius*

Nita Kusumawati[1*], Pirim Setiarso[1], Supari Muslim[2], Nafisatus Zakiyah[1], Khofifatul Rahmawati[1], and Fadlurachman Faizal Fachrirakarsie[1]

[1]*Department of Chemistry, Faculty of Mathematics and Natural Sciences, Universitas Negeri Surabaya, Jl. Ketintang, Surabaya 60231, Indonesia*

[2]*Department of Electrical Engineering, Faculty of Engineering, Universitas Negeri Surabaya, Jl. Ketintang, Surabaya 60231, Indonesia*

* ***Corresponding author:***

email: nitakusumawati@unesa.ac.id

Received: February 2, 2024
Accepted: July 22, 2024

DOI: 10.22146/ijc.93830

Abstract: *This study optimizes dye-sensitized solar cell (DSSC) performance using a combination of natural dye components extracted from* Beta vulgaris *L. (beetroot),* Curcuma longa *L. (turmeric), and* Pandanus amaryllifolius *(pandanus leaf). These plants were selected for their natural pigments—betacyanin, curcuminoids, and chlorophyll—which potentially act as DSSC sensitizers. Dyes were extracted via maceration with ethanol solvent (1:6 sample:solvent ratio) for 24 h. Filtrates were combined in various ratios to test DSSC performance. The optimal C4 dye combination, with a 2:1:1 ratio (betacyanin:curcumin:chlorophyll), demonstrated the best performance. The UV-vis analysis revealed complex interactions and synergistic effects among dye combinations, characterized by increased light absorption in the 400–700 nm range. Cyclic voltammetry analysis showed favorable energy band gap values, confirming the pigments' suitability for DSSC applications. FTIR analysis confirmed the stable coexistence of the three dyes without new bond formation. Photovoltaic performance testing showed the C4 three-dye combination achieved the highest energy conversion efficiency of 3.57%. These results demonstrate the potential of this dye combination to contribute to the development of sustainable and efficient solar energy conversion in DSSCs.*

Keywords: *DSSCs; triple-component blending;* Beta vulgaris *L.;* Curcuma longa *L.;* Pandanus amaryllifolius

■ INTRODUCTION

Global energy needs are on the rise [1]. Based on the estimations provided by the International Energy Agency, there is a projected 45% increase in world energy demand by 2030, equating to an average annual growth rate of 1.6% [2-3]. Approximately 80% of the world's energy needs are supplied by non-renewable energy sources, primarily in the form of fossil fuels [4]. This heightened interest in renewable energy as an eco-friendly option, prompting the exploration of different solar cell technologies [5]. Dye-sensitive solar cells (DSSCs) have garnered great attention for their cost-effectiveness, straightforward manufacturing process, and notable efficiency [6-8].

The principle of DSSC is converting solar energy into electrical energy using photosensitive dyes [9]. DSSC has components such as glass substrate, transparent conducting, TIO_2, electrolyte, counter electrode, and natural dye [10]. This study employs polyvinylidene difluoride nanofiber (PVDF NF) electrolyte membranes due to their significant advantages in stability [11-12], despite a marginal reduction in efficiency compared to liquid electrolytes. The utilization of PVDF NF membrane-based electrolytes represents a strategic choice, emphasizing the importance of enhanced stability in DSSCs, as revealed by the referenced study [13-16].

Natural dyes are gaining prominence as favorable substitutes for synthetic counterparts in DSSC due to their environmental friendliness, low cost, and abundant availability [17-19]. *Beta vulgaris* L., *Curcuma longa* L., and *Pandanus amaryllifolius* are some of the natural sources that have been explored for their potential as sensitizers in DSSC [20-21]. The advantage of each material lies in its optimal absorption of sunlight to produce the best excitation energy [22-23]. The dye absorbs sunlight and generates electrons, which are then collected by the electrodes and transferred to an external circuit [24].

The development of natural dye-based DSSC has significant relevance in today's industry. With the increasing demand for renewable energy sources, alternatives to sustainable and environmentally friendly synthetic dyes are needed. Natural dyes offer a promising solution to this problem, and their use in DSSCs could contribute to developing inexpensive and efficient solar cells. Furthermore, exploring natural sources for dyes may also lead to the discovery of new sensitizers with better properties. Most previous studies have focused on using a single synthetic or natural dye. However, an interesting new approach combines two or more types of natural dyes to be used as photosensitizers in DSSCs.

In this study, we propose the use of a combination of three different types of natural dyes, namely betacyanin from beetroot, curcuminoids from turmeric, and chlorophyll from pandanus leaves, through a three-component mixing approach with different ratio variations. The combination of these natural dyes is expected to broaden the absorption range and synergistically improve the efficiency of DSSC. Detailed characterizations such as UV-vis, cyclic voltammetry, and FTIR were performed to understand the interaction and suitability of the dye combination as a DSSC sensitizer. In addition, the mixing ratio was optimized to achieve the highest photoconversion performance. This approach contributes to developing sustainable and environmentally friendly DSSCs by utilizing easily available natural dye sources. The PVDF NF membrane will trap the dye so that it does not easily escape, thus the absorption results are maximized.

■ EXPERIMENTAL SECTION

Materials

The materials utilized in this research comprised PVDF (Mw ~534,000) and dimethylacetamide (DMAC, ≥ 99.9%) obtained from Sigma Aldrich in Germany. Acetone (≥ 99.5%), nitric acid (HNO_3, ≥ 99.9%), and anatase titanium dioxide powder (TiO_2, ≥ 99.5%, particle size: 21 nm), anhydrous ethylene carbonate (EC, 99%), and propylene carbonate (99.7%) were obtained from Sigma Aldrich in the USA. Polyethylene glycol (PEG) and potassium iodide (KI) have a purity of at least 99% from Merck in Germany. Ethanol (≥ 99.7%), Tween 80, and iodine (≥ 99.8%) were obtained from PT. Smart Lab in Indonesia. Fluorine-doped tin oxide glass (FTO, resistivity 10 Ω) manufactured by XinYu Xu Tking Glass Co., L in China. *Beta vulgaris* L., *Curcuma longa* L., and *Pandanus amaryllifolius* were bought from the local agricultural farm in Surabaya, Indonesia.

Instrumentation

The experimental setup utilized various analytical and laboratory equipments including a Buchi R-300 rotary evaporator for solvent removal and a NESCO LAB MS-H280-Pro magnetic stirrer for mixing solutions. Spectroscopic analysis was conducted using a Shimadzu UV-1800 UV-vis spectrophotometer and a Perkin Elmer Spectrum Two FTIR spectrophotometer. Electrochemical measurements were performed with a 797 VA Computrace Metrohm voltammetry system. Electrical parameters were measured using a Krisbow KW08-267 multimeter.

Procedure

Preparation of the natural dyes

Preparing organic photosensitizers through maceration follows a similar approach [12]. Each natural dye, namely *B. vulgaris* L., *C. longa* L., and *P. amaryllifolius*, was obtained and subsequently washed with water. After cleaning, each dye was extracted using the maceration method with ethanol solvent at a ratio of 1:6 (sample to solvent) for 24 h. The filtrate of each natural dye was combined in the following ratio to achieve a total amount of 50 mL. Different combinations

of dyes were prepared by combining these dyes at varying volume ratios: A1 (100% red), A2 (100% yellow), A3 (100% green), B1 (50% red + 50% yellow), B2 (50% yellow + 50% green), B3 (50% red + 50% green), C1 (60% red + 30% yellow + 10% green), C2 (30% red + 10% yellow + 60% green), C3 (10% red + 60% yellow + 30% green), C4 (50% red + 25% yellow + 25% green), C5 (25% red + 50% yellow + 25% green), and C6 (25% red + 25% yellow + 50% green). All twelve dye combinations were utilized as sources of dye sensitizers for DSSC.

PVDF NF membrane manufacturing

The production of PVDF membranes was performed using electrospinning techniques, following the established procedures [14].

Preparation of electrolyte

In the formulation process, 0.60 g of KI, 0.09 g of I_2, 4.00 g of PC, and 4.00 g of EC were stirred at 100 rpm for 1 h. This resulting solution, serving as the electrolyte, was meticulously stored in an opaque container to protect it from light exposure, ensuring optimal stability for subsequent applications.

TiO_2 paste preparation

The TiO_2 paste was meticulously prepared in accordance with the procedure established in a prior study [14]. In this process, 0.40 g of TiO_2 was combined with 0.16 g of PEG 1000. The mixture was further enriched with 0.10 mL of HNO_3 and 0.80 mL of Tween 80, undergoing thorough stirring for approximately 30 min at 100 rpm to ensure even dispersion. Subsequently, the prepared TiO_2 paste, utilizing the doctor blade method, was applied onto the FTO anode with a 3.00 cm^2 active area and TiO_2 0.20 mm of thickness. The coated substrate underwent sintering at 450 °C for 1 h, resulting in a well-defined product.

Fabrication DSSC

After sintering, the TiO_2 photoanode undergoes immersion in a 10 mL solution of natural dye for 24 h. Subsequently, a precisely cut PVDF membrane, fabricated through a combination of casting and electrospinning methods, measures 2.0 cm in length and 1.5 cm in width. The membrane is immersed in 1.0 mL of electrolyte for 1 h. The cathode on an FTO glass substrate receives a carbon coating derived from a candle. The configuration of the DSSC circuit is defined as FTO/TiO_2/PVDF/Pt/FTO. The construction process of DSSC can be seen in Fig. 1.

Characterization of DSSC

The absorption spectra of dye pigments within the DSSC were analyzed using UV-vis. Changes in both the current and potential associated with the color pigment

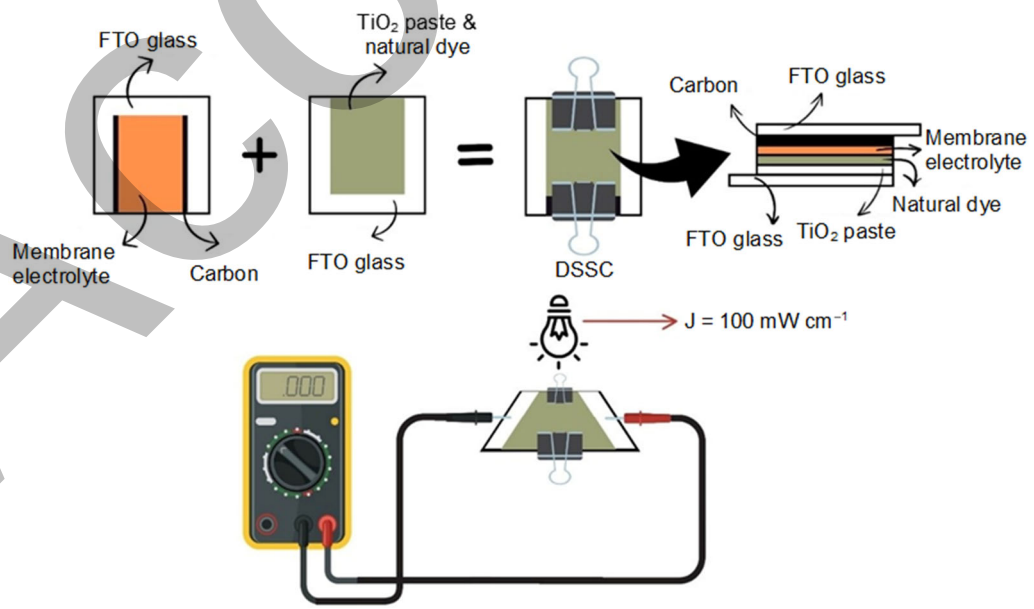

Fig 1. Diagram depicting the construction process of the DSSC

used in the DSSC were assessed utilizing a 797 VA Computrace Metrohm. Functional groups in the pigments were identified through the application of a FTIR spectrophotometer. The current and voltage were measured using a multimeter to assess the performance of the DSSC circuit.

■ RESULTS AND DISCUSSION

UV-vis Analysis

In the context of DSSC, the dye plays an important role by enhancing the absorption of the visible light spectrum on TiO_2. Natural dyes present several advantages over synthetic counterparts, as they are more readily available, cost-effective, require fewer chemical operations for extraction, possess a high absorption coefficient, and exhibit non-toxic and biodegradable properties [25]. Evaluating the potential of blending the three dyes from *B. vulgaris* L. (red dye), *C. longa* L. (yellow dye), and *P. amaryllifolius* (green dye) as natural dyes in DSSC involved a thorough examination using a UV-vis spectrophotometer, focusing on visible light wavelengths within the range of 400–750 nm.

This study delves into the optical properties of three dyes extracted from beetroot, turmeric, and pandanus, utilizing ethanol as the solvent. The research significantly contributes to understanding the intricate characteristics emerging from the blending dyes of beetroot, turmeric, and pandanus dyes, which are essential for their potential use as natural sensitizers in DSSC. The investigation includes a meticulous determination of wavelengths for

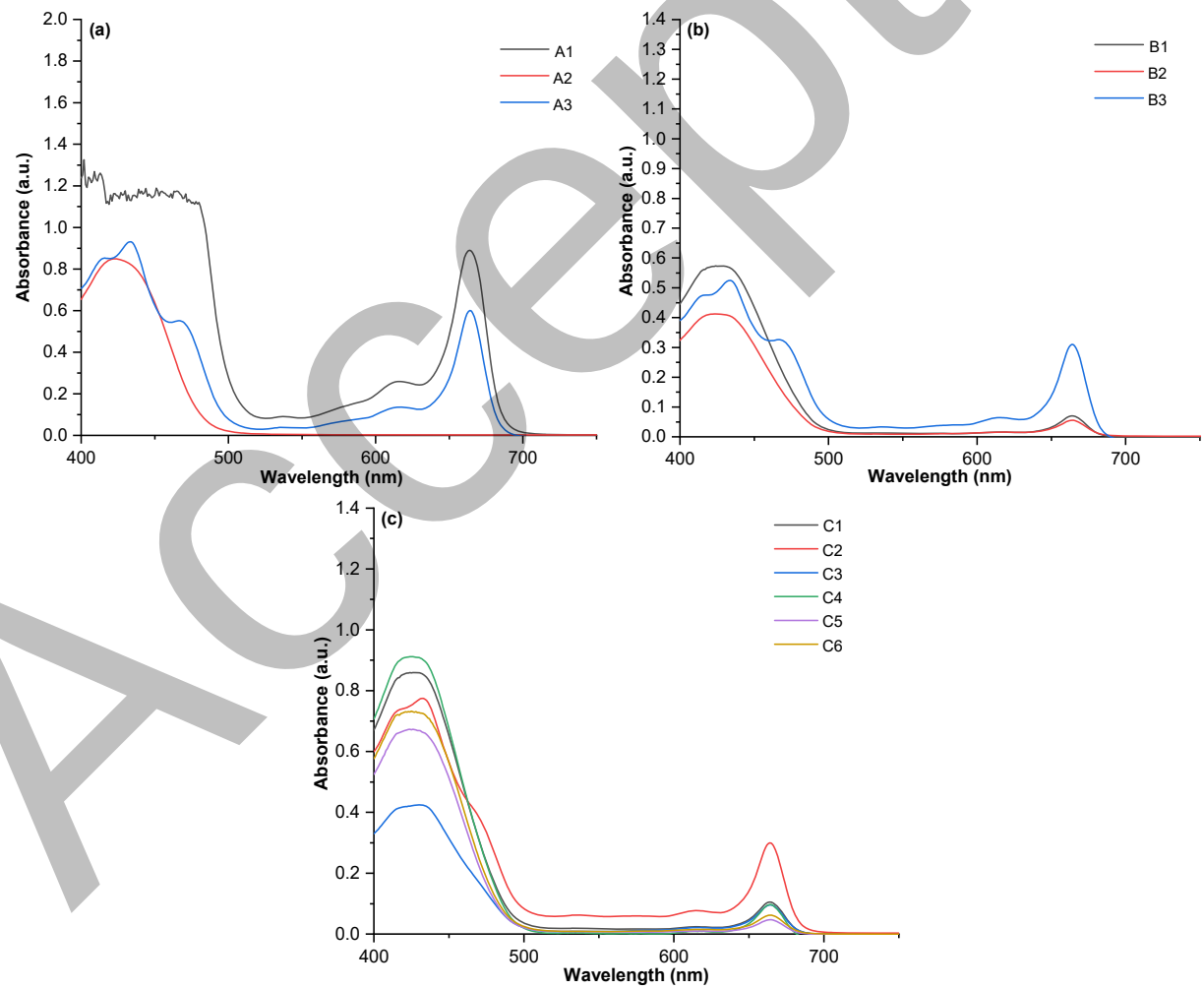

Fig 2. UV-vis spectrum of a) each single dye (red, yellow, and green), b) double blending of two dyes, and c) triple component blending of three dyes

each dye combination, offering pivotal insights into the initial characterization of these blends.

Fig. 2(a) illustrates the highest absorption peaks for individual dyes, namely beetroot (red dye), curcumin (yellow dye), and pandanus (green dye), within the wavelength range of 400–750 nm. The peak wavelengths are recorded as 532 nm for betacyanin (A1), 424 nm for curcumin (A2), and 433 and 664 nm for pandanus (A3). Betacyanin, found in *B. vulgaris* L., is soluble in common polar solvents like water, ethanol, and methanol [26-27], exhibiting an absorption wavelength range of 480–540 nm [28]. Notably, a strong absorption peak at 532 nm has been observed, as reported by Devadiga et al. [29]. Turmeric, known for its diverse applications, has been explored as a natural dye due to the presence of the curcumin pigment [30]. Curcumin, the primary compound in turmeric extract, imparts a vivid yellow color [31]. The absorption spectrum of curcumin spans the critical wavelength range of 350–470 nm. In comparison, chlorophyll *P. amaryllifolius* exhibits two absorption peaks at 434 and 664 nm, as reported in the study by Ishak et al. [32].

The absorption characteristics of the double-blending dye are illustrated in Fig. 2(b), where the synergistic effects of dual dye combinations are evident. Notably, the double blending of beetroot and turmeric dye (designated as B1), the combination of turmeric and pandanus dye (B2), and the amalgamation of beetroot with pandanus (B3) dye collectively exhibit pronounced absorption peaks within the wavelength range of 400–700 nm. The specific peak wavelengths for these combinations are measured as follows: 664.13 nm for B1; 664.53 nm for B2; and 664.21 nm for B3. These outcomes underscore the intricate interplay of natural dyes and illuminate their potential for applications across diverse wavelength-sensitive domains in DSSCs. Meanwhile, in Fig. 2(c), the wavelength characteristics of three dyes were investigated, revealing the highest absorption peak in their combined composition. This combination was further varied through six distinct compositions (C1–C6), and each variation was meticulously characterized within the wavelength range of 400–700 nm. The amalgamation of the three dyes yielded analogous wavelengths, unveiling two prominent peaks observed at 664 and 426–430 nm. The absorption spectrum in the wavelength range above 400 nm is influenced by nine conjugated double (C=C) bonds. The C=C bond is responsible for the electron transfer from n to π^*, as shown in the peak at 400–700 nm. Meanwhile, the peak at 430 nm is associated with the electron transition from n to π^*, originating from the carbonyl group (C=O) [33].

The improved cumulative light absorption observed in the UV-vis spectrum indicates that the combinations of all dyes absorb light more effectively than a single dye, as evidenced by higher absorbance. These findings show potential applications of these blends as sensitizers in DSSC, showcasing the viability of solar energy conversion systems. In addition, the stability of the absorption characteristics of each dye in the blend indicates good compatibility between these dyes, which is crucial for the long-term performance of the solar cell.

Voltammetry Cyclic Analysis

In the pursuit of elevating the overall efficiency of DSSC and optimizing the efficacy of natural dyes as photosensitizers, it is crucial that the band gap energy of the dye is narrower than that of the semiconductor TiO_2. The efficacy of the extracted dye improves as the disparities between the highest occupied molecular orbital (HOMO) and the lowest unoccupied molecular orbital (LUMO) values decrease. The dye's capacity to regenerate shows how easily electrons may go from the I^- or I_3^- electrolyte to the substance's HOMO band [34]. This has to do with the fact that dye electrons can be stimulated more easily from the valence band to the conduction band when they have a tiny enough amount of energy. TiO_2 exerts influence on the conduction band, aligning its impact with the energy level of the LUMO dye molecule and facilitating electron injection. In particular, the anatase phase exhibits a band gap energy of 3.2 eV, whereas the rutile phase manifests a slightly lower value at 3.0 eV. The determination of the dye's band gap energy relies upon the subsequent Eq. (1–3) [35]:

$$E_{HOMO} = -\left(E_{ox} + 4.40\right)eV \quad (1)$$

$$E_{LUMO} = -(E_{red} + 4.40)eV \quad (2)$$

$$E_g = E_{LUMO} - E_{HOMO} \quad (3)$$

Based on the energy band gap values obtained for each dye with the various compositions, it shows that triple component blending pigments can be used as sensitizers in DSSC because they meet the requirements of DSSC dyes (Table 1). The LUMO values of each dye are significantly higher than the conduction value of TiO_2. It is essential for the dye to fulfill the requirement of having a sufficiently high LUMO level compared to the conduction band of the TiO_2 semiconductor, which is −4.0 eV, which ensures the capability of electron injection from the excited dye into the semiconductor [36].

Fig. 2 shows that each combination of dyes has energy gaps between 0.1309 and 0.7003 eV. Notably, the three-component blending exhibits the smallest energy gap, followed by the two-component blending and single-dye without blending. The specific composition variation C4 (2:1:1) stands out as having the most favorable energy gap within the study, with a band gap value of 0.1309 eV. This indicates the suitability and stability of the dye mixture for DSSC applications. This smaller band gap facilitates more efficient electron transfer, which is important for long-term DSSC performance. A reduced band gap implies a narrower energy difference between the valence and conduction bands, facilitating the movement of electrons and enhancing electrical conductivity [37].

Table 1. The HOMO, LUMO, and band gap values for diverse dye combinations

Dye (composition)		HOMO (eV)	LUMO (eV)	Eg (eV)
A	(1) 1:0:0	−4.2543	−3.7061	0.5482
	(2) 0:1:0	−4.2801	−3.5798	0.7003
	(3) 0:0:1	−4.2862	−3.8441	0.4421
B	(1) 1:1:0	−4.1562	−3.7241	0.4321
	(2) 0:1:1	−4.1990	−3.8231	0.3759
	(3) 1:0:1	−4.2963	−3.9511	0.3452
C	(1) 6:3:1	−4.2584	−4.0503	0.2081
	(2) 3:1:6	−4.1069	−3.9357	0.1712
	(3) 1:6:3	−4.0742	−3.9204	0.1538
	(4) 2:1:1	−4.0868	−3.9559	0.1309
	(5) 1:2:1	−4.0693	−3.9132	0.1561
	(6) 1:1:2	−4.2085	−3.9654	0.2431

The lower energy gap promotes a shift towards longer wavelengths in the absorption spectrum, known as a bathochromic shift, which is advantageous for improving the efficiency of photovoltaic devices [38].

FTIR Analysis

The investigation extended to analyzing functional groups within the extracted dyes using FTIR spectroscopy. The outcomes are depicted in Fig. 3, wherein the respective FTIR spectra for each dye with varied combinations are presented.Based on Fig. 3, all the dyes show very similar transmission wavenumber spectra ranging from 4000 to 500 cm^{-1} C–Cl stretching, indicating the presence of alkyl halides at 803.17 cm^{-1}. The C–H bending indicates the presence of alkenes at 1087.28 cm^{-1}. The broad absorption band at wave numbers 600–900 cm^{-1} indicates the presence of C–H bending vibrations of unsaturated alkenes. The C–O stretching indicates the presence of ether at 1044.88 cm^{-1} [39]. The 1416.91 cm^{-1} peak in the C=C stretching region signifies the existence of aromatic compounds. Additionally, the distinct absorption band at 1710 cm^{-1} points to the presence of C=O stretching vibrations, indicative of compounds such as ketones, aldehydes, carboxylic acids, or esters. The ability of the chromophore groups in chlorophyll pigments, such as the C=O group, to absorb light in the visible spectrum of sunlight is responsible for enhancing solar efficiency when utilizing natural pigments [40]. When exposed to visible light, the current density is often lower than that induced by UV light. This indicates that TiO_2 exhibits a strong response in the UV region. The increased current suggests the presence of electron excitation [41]. The C=C stretching observed at 1651.60 cm^{-1} denotes the existence of alkenes or the primary N–H bending vibrations characteristic of amides. The C–H stretching (asymmetric) indicates the presence of alkanes at 2974.49 cm^{-1}. The wavenumbers at 3338.08 cm^{-1} indicate the presence of alcohols that occur in O–H stretching vibrations from O–H in alcohols or carboxylic acids [15,42].

The O–R bond vibrations generally give absorption in the 1300–1000 cm^{-1} region. However, this

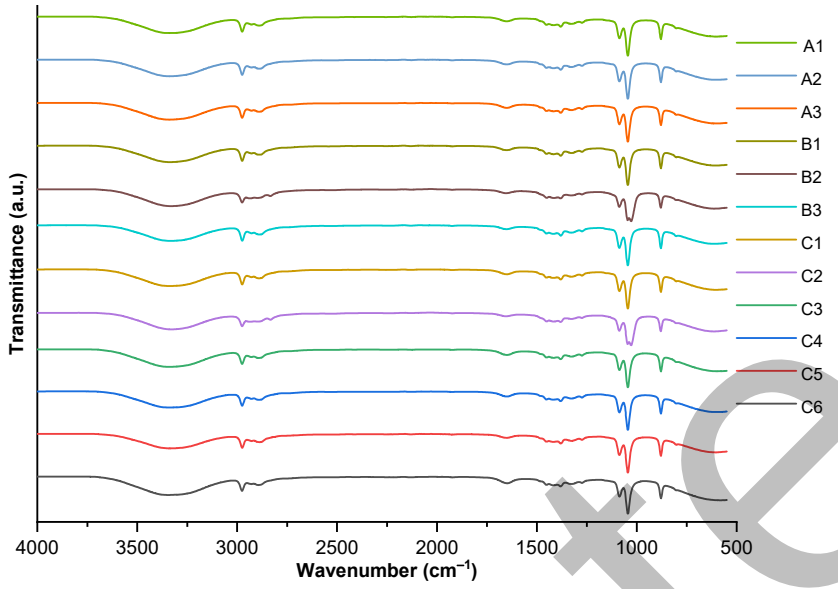

Fig 3. FTIR spectra of each single dye (A1-A3), double blending of two dyes (B1-B3), and triple component blending of three dyes (C1-C6)

FTIR graph has no significant sharp absorption band in the wavenumber region. This is due to several factors, including the absence of O–R functional groups in the analyzed compounds, the concentration of O–R groups appearing too small to be detected, and their overlap with the absorption bands of other functional groups so that the O–R signal does not appear as a separate band. The position of the O–R bond is not symmetrical, so the absorption is weak and "drowned" by other bands. Based on this, it can be concluded that the possibility that this compound does not contain O–R functional groups, or even if it exists, the concentration is so small that it is not detected in this FTIR spectrum. Analysis of the FTIR spectra revealed that the amalgamation of the three natural dyes did not form any novel chemical bonds. The spectra showed that these dyes simply coexisted without reacting with each other, indicating good chemical stability in the mixture. The absence of significant new peaks or large shifts in the existing peaks corroborates the conclusion that these dyes are compatible with the mixture. It is reasonable to suspect that when these natural dyes are combined, they simply coexist without reacting [43-44].

Photovoltaic Studies

The assessment of the DSSC circuit, organized to measure open voltage (V_{oc}), short-circuit current (J_{sc}), fill factor (FF), and efficiency (η), is conducted utilizing a multimeter under illumination from a lamp with an intensity of 100 mW/cm^2. The overall cell performance is determined by the FF (Eq. (4)) and cell efficiency (η) (Eq. (5)) is performed according to the formula referenced by Kusumawati et al. [14]:

$$FF = \frac{V_{max} \times I_{max}}{V_{oc} \times I_{sc}} \quad (4)$$

$$\eta = \frac{FF \times V_{oc} \times I_{sc}}{P_{in}} \quad (5)$$

where V_{max} represents the maximum output voltage, I_{max} denotes the maximum output current, I_{sc} signifies the short circuit current, V_{oc} indicates the open circuit voltage, and P_{in} denotes the input power.

This study examines the current-voltage (I-V) characteristics of DSSCs, employing red dye (betacyanin), yellow dye (curcumin), and green dye (chlorophyll) with various combinations. DSSC performance is evaluated through V_{oc}, I_{sc}, and FF. The impact of utilizing blends of these natural photosensitizers on DSSC performance is evident in the I-V curves (Fig. 4) and the photovoltaic characterization presented in Table 2.

The efficacy of integrating natural pigments like betacyanin, curcumin, and chlorophyll derived from beetroot, turmeric, and pandanus holds promise as photosensitizers in DSSC. These three pigment types can

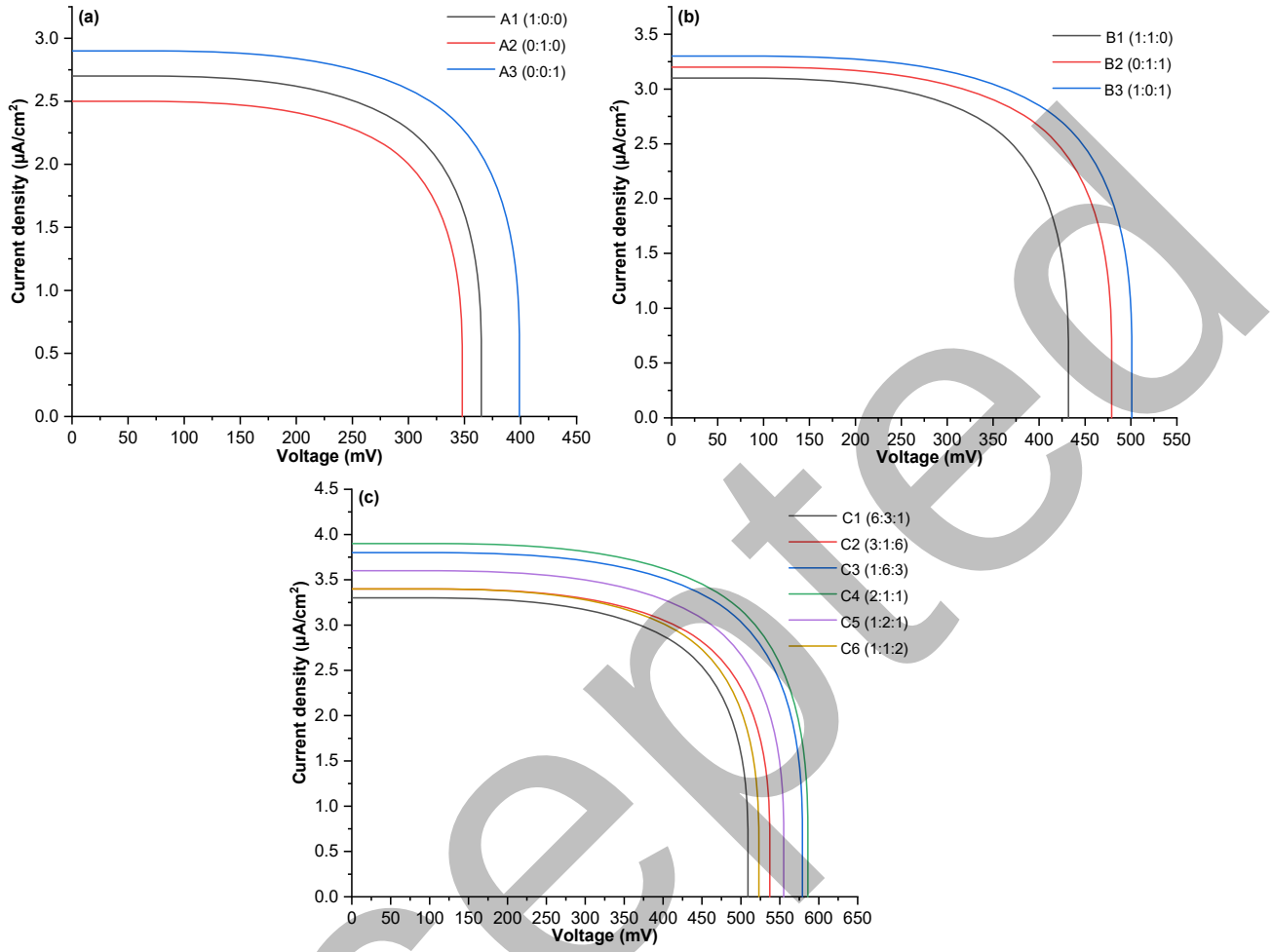

Fig 4. Photocurrent–voltage curves were obtained for DSSC sensitized of a) each single dye (red, yellow, and green), b) double blending of two dyes, and c) triple component blending of three dyes

Table 2. Photovoltaic parameters of DSSC

Dye (various composition)		V_{oc} (mV)	I_{sc} (mA/cm²)	FF (%)	Efficiency (%)
A	(1) 1:0:0	365	0.0027	3.05	1.01
	(2) 0:1:0	348	0.0025	3.18	1.93
	(3) 0:0:1	399	0.0029	3.77	1.46
B	(1) 1:1:0	432	0.0031	3.46	1.55
	(2) 0:1:1	479	0.0032	3.51	1.74
	(3) 1:0:1	501	0.0033	3.86	2.13
C	(1) 6:3:1	509	0.0033	3.95	2.21
	(2) 3:1:6	537	0.0034	4.13	2.51
	(3) 1:6:3	579	0.0038	4.99	3.03
	(4) 2:1:1	586	0.0039	4.69	3.57
	(5) 1:2:1	555	0.0036	3.82	2.55
	(6) 1:1:2	523	0.0034	4.03	2.39

capture light at distinct wavelengths suitable for the DSSC mechanism, converting photons into electricity. The utilization of triple-component blending extends the range of absorbed sunlight, potentially enhancing DSSC efficiency. Additionally, as photosensitizers, these pigments demonstrate commendable chemical and photochemical stability.

Among the twelve variations in dye combinations tested, the efficiency order observed was C (triple-component blending) > B (double-component blending) > A (no blending) with the most effective triple-component blending combination was C4 (2:1:1). The C4 dye exhibited values for I_{sc}, V_{oc}, FF, and η of 0.39 mA/cm^2, 0.586 V, 5.29, and 3.57%, respectively. This achievement shows that the dye mixture remains stable and effective under the operational conditions of the DSSC. In addition, this alignment with the previous band gap analysis indicates that the C4 (2:1:1) dye has a smaller band gap. Smaller band-gap values signify faster electron transfer due to an increased number of conjugated chains [45]. The band gap data reveal that the C4 (2:1:1) dye has the smallest band gap among composition variations, leading to enhanced performance attributed to increased absorption of solar light and more efficient utilization of photon energy [46]. In addition, the increase in DSSC efficiency is also influenced by the optimal TiO_2 thickness of 0.2 mm and the optimal PVDF NF polymer electrolyte membrane, as reported by Kusumawati et al. [14].

The combination of three different natural dyes – betacyanin from *B. vulgaris* L., curcuminoid from *C. longa* L., and chlorophyll from *P. amaryllifolius*, led to a significant increase in solar cell performance. This can be attributed to the distinct chemical structures and properties of these dye molecules. Fig. 5 shows betacyanins have carboxyl and O–H groups that can chelate to the TiO_2 surface, improving dye adsorption and electronic coupling for efficient electron transfer. Fig. 6 shows curcuminoid contains phenolic groups and C=C bonds, making it highly polar and allowing efficient light absorption. The keto-enol tautomerism in curcuminoid facilitates intramolecular charge transfer and stabilizes the excited state, aiding electron injection into TiO_2. Fig. 7 shows chlorophyll possesses a porphyrin ring structure that enables absorption in the 600–700 nm range.

However, the alkyl side chains make it difficult to form strong chemical bonds with TiO_2, limiting electron injection efficiency. When these three dyes are combined, their complementary absorption spectra result

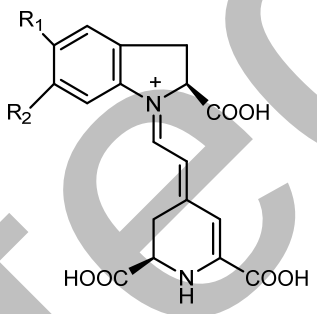

Fig 5. The chemical structure of betacyanin

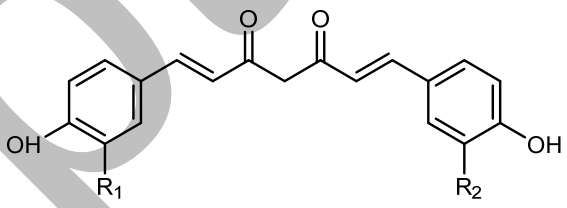

Fig 6. The chemical structure of curcuminoid

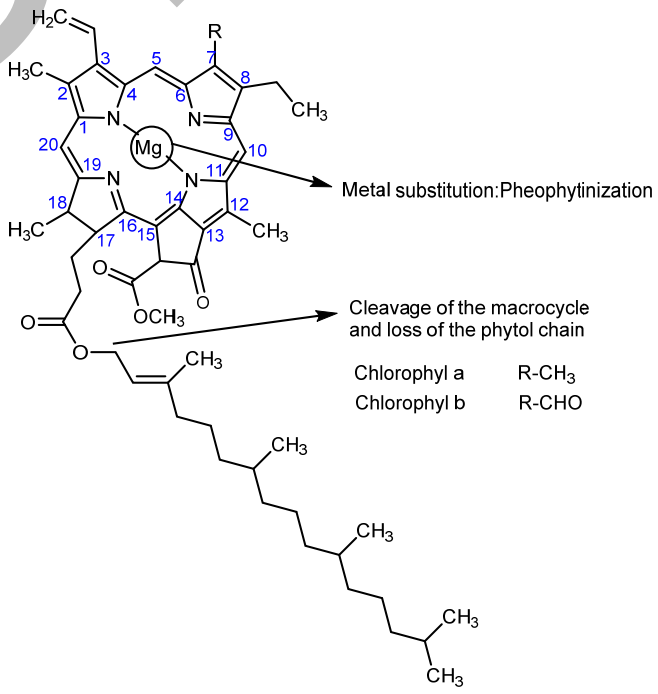

Fig 7. The chemical structure of chlorophyll

in a broader spectral coverage from 300–700 nm, harvesting more photons [47]. Additionally, the presence of anchoring groups like carboxylates and phenolics facilitates dye binding to TiO_2 and promotes charge injection/regeneration kinetics. The synergistic effect of combining curcuminoid's charge transfer capability, chlorophyll's red-light absorption, and anthocyanin's anchoring ability overcome the individual limitations, leading to improved light harvesting, charge separation, and overall device performance in the triple-dye system compared to single dye cells.

■ CONCLUSION

This study used a combination of three natural dyes from *B. vulgaris* L., *C. longa* L., and *P. amaryllifolius* extracts as a dye-sensitizer of DSSC. UV-vis analysis showed the interaction of the combination of the three dye mixtures, characterized by an increase in absorption peaks at 664 and 426–430 nm. Cyclic voltammetry analysis also showed a favorable decrease in the band gap energy in the C4 (2:1:1) composition with the band gap energy 0.1309 eV, indicating an increase in electron injection and electrical conductivity. FTIR analysis confirmed the coexistence of the three dyes without forming new bonds that could affect stability. Photovoltaic studies showed the best performance on the three-component dye combination C4 (2:1:1) with the highest conversion efficiency (η) of 3.57%, exceeding the use of a single dye, indicating its potential in the development of sustainable and efficient solar energy conversion in DSSCs. The results of this study demonstrate the potential of the combination of natural dyes from beetroot, turmeric, and pandan leaves to improve the performance of DSSCs and contribute to the development of environmentally friendly solar cells.

■ ACKNOWLEDGMENTS

The author expresses gratitude to the Ministry of Education, Culture, Research, and Technology of the Republic of Indonesia for the financial support extended through national competitive research grants with contract number B/61614/UN38.III.1/LK.04.00/2024.

■ CONFLICT OF INTEREST

The authors have no conflict of interest.

■ AUTHOR CONTRIBUTIONS

Nita Kusumawati contributed to the conceptualization, formal analysis, methodology, and investigation. Nita Kusumawati, Pirim Setiarso and Nafisatus Zakiyah were responsible for conducting the experiments, performing calculations (data processing), providing resources, reviewing, and editing the manuscript. Supari Muslim contributed as the DSSC circuit designer. Nafisatus Zakiyah, Khofifatul Rahmawati, and Fadlurachman Faizal Fachrirakarsie played a role in drafting and revising the manuscript. All authors participated in reading and approving the final version of the manuscript.

■ REFERENCES

[1] Abu-Rayash, A., and Dincer, I., 2020, Analysis of the electricity demand trends amidst the COVID-19 coronavirus pandemic, *Energy Res. Social Sci.*, 68, 101682.

[2] Aktar, M.A., Alam, M.M., and Al-Amin, A.Q., 2021, Global economic crisis, energy use, CO_2 emissions, and policy roadmap amid COVID-19, *Sustainable Prod. Consumption*, 26, 770–781.

[3] Koot, M., and Wijnhoven, F., 2021, Usage impact on data center electricity needs: A system dynamic forecasting model, *Appl. Energy*, 291, 116798.

[4] Amin, M., Shah, H.H., Fareed, A.G., Khan, W.U., Chung, E., Zia, A., Rahman Farooqi, Z.U., and Lee, C., 2022, Hydrogen production through renewable and non-renewable energy processes and their impact on climate change, *Int. J. Hydrogen Energy*, 47 (77), 33112–33134.

[5] Shubbak, M.H., 2019, Advances in solar photovoltaics: Technology review and patent trends, *Renewable Sustainable Energy Rev.*, 115, 109383.

[6] Shashanka, R., Esgin, H., Yilmaz, V.M., and Caglar, Y., 2020, Fabrication and characterization of green synthesized ZnO nanoparticle based dye-sensitized

solar cells, *J. Sci.: Adv. Mater. Devices*, 5 (2), 185–191.

[7] Orhan, E., Gökçen, M., and Taran, S., 2021, Effect of the photoanode fabrication condition, electrolyte type and illumination type on dye-sensitized solar cells performance, *Bull. Mater. Sci.*, 44 (1), 60.

[8] Özaydın, C., and Gözel, M., 2023, The use of copper-quercetin complex as photosensitizer in dye sensitive solar cells and its photovoltaic performance, *Braz. J. Phys.*, 53 (1), 28.

[9] Zhang, C., Zhang, J., Ma, X., and Feng, Q., 2021, "Dye-Sensitized Solar Cell" in *Semiconductor Photovoltaic Cells*, Springer Singapore, Singapore, 325–372.

[10] Weldemicheal, H.T., Desta, M.A., and Mekonnen, Y.S., 2023, Derivatized photosensitizer for an improved performance of the dye-sensitized solar cell, *Results Chem.*, 5, 100838.

[11] Kusumawati, N., Setiarso, P., Muslim, S., and Purwidiani, N., 2018, Synergistic ability of PSf and PVDF to develop high-performance PSf/PVDF coated membrane for water treatment, *Rasayan J. Chem.*, 11 (1), 260–279.

[12] Kusumawati, N., Setiarso, P., Santoso, A.B., Muslim, S., A'yun, Q., and Putri, M.M., 2023, Characterization of poly(vinylidene fluoride) nanofiber-based electrolyte and its application to dye-sensitized solar cell with natural dyes, *Indones. J. Chem.*, 23 (1), 113–126.

[13] Kusumawati, N., Setiarso, P., and Muslim, S., 2018, Polysulfone/polyvinylidene fluoride composite membrane: Effect of coating dope composition on membrane characteristics and performance, *Rasayan J. Chem.*, 11 (3), 1034–1041.

[14] Kusumawati, N., Setiarso, P., Muslim, S., Hafidha, Q.A., Cahyani, S.A., and Fachrirakarsie, F.F., 2024, Optimization thickness of photoanode layer and membrane as electrolyte trapping medium for improvement dye-sensitized solar cell performance, *Sci. Technol. Indones.*, 9 (1), 7–16.

[15] Bashar, H., Bhuiyan, M.M.H., Hossain, M.R., Kabir, F., Rahaman, M.S., Manir, M.S., and Ikegami, T., 2019, Study on combination of natural red and green dyes to improve the power conversion efficiency of dye sensitized solar cells, *Optik*, 185, 620–625.

[16] Zakiyah, N., Kusumawati, N., Setiarso, P., Muslim, S., A'yun, Q., and Putri, M.M., 2024, Characterization and application of natural photosensitizer and poly(vinylidene fluoride) nanofiber membranes-based electrolytes in DSSC, *Indones. J. Chem.*, 24 (3), 701–714.

[17] Theerthagiri, J., Murthy, A.P., Lee, S.J., Karuppasamy, K., Arumugam, S.R., Yu, Y., Hanafiah, M.M., Kim, H.S., Mittal, V., and Choi, M.Y., 2021, Recent progress on synthetic strategies and applications of transition metal phosphides in energy storage and conversion, *Ceram. Int.*, 47 (4), 4404–4425.

[18] Peter, S., Lyczko, N., Gopakumar, D., Maria, H.J., Nzihou, A., and Thomas, S., 2021, Chitin and chitosan based composites for energy and environmental applications: A review, *Waste Biomass Valorization*, 12 (9), 4777–4804.

[19] Srivastava, A., Singh Chauhan, B., Chand Yadav, S., Kumar Tiwari, M., Akash Kumar Satrughna, J., Kanwade, A., Bala, K., and Shirage, P.M., 2022, Performance of dye-sensitized solar cells by utilizing *Codiaeum variegatum* leaf and *Delonix regia* flower as natural sensitizers, *Chem. Phys. Lett.*, 807, 140087.

[20] Darmawan, M.I., Hardani, H., Halid, I., Aini, A., Ustiawaty, J., and Fardani, RA, 2023, Fabrication of dye-sensitized solar cells (DSSC) using *Pandanus amaryllifolius* extract, *AIP Conf. Proc.*, 2623 (1), 030002.

[21] Estiningtyas, I.W., Kusumawati, N., Setiarso, P., Muslim, S., Rahayu, N.T., Safitri, R.N., Zakiyah, N., and Fachrirakarsie, F.F., 2023, Effect of natural dye combination and pH extraction on the performance of dye-sensitized photovoltaics solar cell, *Int. J. Renewable Energy Dev.*, 12 (6), 1054–1060.

[22] Teja, A.S., Srivastava, A., Satrughna, J.A.K., Tiwari, M.K., Kanwade, A., Chand Yadav, S., and Shirage, P.M., 2023, Optimal processing methodology for

futuristic natural dye-sensitized solar cells and novel applications, *Dyes Pigm.*, 210, 110997.

[23] Prakash, P., and Janarthanan, B., 2023, Review on the progress of light harvesting natural pigments as DSSC sensitizers with high potency, *Inorg. Chem. Commun.*, 152, 110638.

[24] Ibrahim, I., Lim, H.N., Wan, N.W.K., Huang, N.M., Lim, S.P., Busayaporn, W., and Nakajima, H., 2021, Plasmonic silver sandwich structured photoanode and reflective counter electrode enhancing power conversion efficiency of dye-sensitized solar cell, *Sol. Energy*, 215, 403–409.

[25] Mejica, G.F., Ramaraj, R., and Unpaprom, Y., 2022, Natural dye (chlorophyll, anthocyanin, carotenoid, flavonoid) photosensitizer for dye-sensitized solar cell: A review, *Maejo Int. J. Energy Environ. Commun.*, 4 (1), 12–22.

[26] Udonkang, M.I., Inyang, I.J., Ukorebi, A.N., Effiong, F., Akpan, U., and Bassey, I.E., 2018, Spectrophotometry, physiochemical properties, and histological staining potential of aqueous and ethanol extracts of beetroot on various tissues of an albino rat, *Biomed. Hub*, 3 (3), 1–10.

[27] Gengatharan, A., Dykes, G., and Choo, W.S., 2021, Betacyanins from *Hylocereus polyrhizus*: Pectinase-assisted extraction and application as a natural food colourant in ice cream, *J. Food Sci. Technol.*, 58 (4), 1401–1410.

[28] Nouairi, M.E.A., Freha, M., and Bellil, A., 2021, Study by absorption and emission spectrophotometry of the efficiency of the binary mixture (ethanol-water) on the extraction of betanin from red beetroot, *Spectrochim. Acta, Part A*, 260, 119939.

[29] Devadiga, D., and Ahipa, T.N., 2020, "Betanin: A Red-Violet Pigment - Chemistry and Applications" in *Chemistry and Technology of Natural and Synthetic Dyes and Pigments*, Eds. Samarta, A.K., Awwad, N.S., and Algarni, H.M., IntechOpen, Rijeka, Croatia.

[30] El-Saadony, M.T., Yang, T., Korma, S.A., Sitohy, M., Abd El-Mageed, T.A., Selim, S., Al Jaouni, S.K., Salem, H.M., Mahmmod, Y., Soliman, S.M., Mo'men, S.A.A., Mosa, W.F.A., El-Wafai, N.A., Abou-Aly, H.E., Sitohy, B., Abd El-Hack, M.E., El-Tarabily, K.A., and Saad, A.M., 2023, Impacts of turmeric and its principal bioactive curcumin on human health: Pharmaceutical, medicinal, and food applications: A comprehensive review, *Front. Nutr.*, 9, 1040259.

[31] Sharifi-Rad, J., El Rayess, Y., Rizk, A.A., Sadaka, C., Zgheib, R., Zam, W., Sestito, S., Rapposelli, S., Neffe-Skocińska, K., Zielińska, D., Salehi, B., Setzer, W.N., Dosoky, N.S., Taheri, Y., El Beyrouthy, M., Martorell, M., Ostrander, E.A., Suleria, H.A.R., Cho, W.C., Maroyi, A., and Martins, N., 2020, Turmeric and its major compound curcumin on health: Bioactive effects and safety profiles for food, pharmaceutical, biotechnological and medicinal applications, *Front. Pharmacol.*, 11, 01021.

[32] Ishak, N., Salleh, H., Dagang, A.N., Salisa, A.R., Kamarulzaman, N.H., Ghazali, S.M., Abd Majid, S., and Ahmad, Z., 2019, Hybrid solar cell using conjugated chlorophyll from *Pandanus amaryllifoliud* as photosensitizers, *Int. J. Recent Technol. Eng.*, 8 (4), 10142–10147.

[33] Rahmalia, W., Septiani, S., Naselia, U.A., Usman, T., Silalahi, I.H., and Mouloungui, Z., 2021, Performance improvements of bixin and metal-bixin complexes sensitized solar cells by 1-methyl-3-propylimidazolium iodide in electrolyte system, *Indones. J. Chem.*, 21 (3), 669–678.

[34] Makangara, J.J., Sahini, M.G., and Surendra babu, N., 2024, Theoretical and conceptual framework to design D-π-A type organic dyes for application dye-sensitized solar cells, *J. Indian Chem. Soc.*, 101 (2), 101118.

[35] Setiarso, P., Harsono, R.V., and Kusumawati, N., 2023, Fabrication of dye sensitized solar cell (DSSC) using combination of dyes extracted from curcuma (*Curcuma xanthorrhiza*) rhizome and binahong (*Anredera cordifolia*) leaf with treatment in pH of the extraction, *Indones. J. Chem.*, 23 (4), 924–936.

[36] Kabir, F., Bhuiyan, M.M.H., Hossain, M.R., Bashar, H., Rahaman, M.S., Manir, M.S., Ullah, S.M., Uddin, S.S., Mollah, M.Z.I., Khan, R.A., Huque, S., and Khan, M.A., 2019, Improvement of efficiency of dye sensitized solar cells by optimizing the

combination ratio of natural red and yellow dyes, *Optik*, 179, 252–258.

[37] Zang, Y., Chen, L., Zhou, J., Xu, R., and Liu, Z., 2021, Enhanced light utilization in semitransparent organic solar cells based on a nonfullerene acceptor of IEICO-4F, *Appl. Phys. A Mater. Sci. Process*, 127 (11), 889.

[38] Afolabi, S.O., Semire, B., and Idowu, M.A., 2021, Electronic and optical properties' tuning of phenoxazine-based D-A_2-π-A_1 organic dyes for dye-sensitized solar cells. DFT/TDDFT investigations, *Heliyon*, 7 (4), e06827.

[39] Kusumawati, N., Setiarso, P., Sianita, M.M., and Muslim, S., 2018, Transport properties, mechanical behavior, thermal and chemical resistance of asymmetric flat sheet membrane prepared from PSf/PVDF blended membrane on gauze supporting layer, *Indones. J. Chem.*, 18 (2), 257–264.

[40] Sari, P.L., Munawaroh, H., Wahyuningsih, S., and Ramelan, A.H., 2020, Structure and optical properties of Al-doped ZnO nanodrums as anti-reflection coating material in solar cells, *Indones. J. Chem.*, 20 (1), 54–59.

[41] Suharyadi, S., Syauqi, M.I., Amelia, P., Yunita, Y., and Gunlazuardi, J., 2023, Dye-Sensitized solar cell photoelectrochemical tandem system performance study: TiO_2 nanotube/N719, $BiVO_4$/TiO_2 nanotube, Ti^{3+}/TiO_2 nanotube for nitrogen reduction reaction to ammonia, *Indones. J. Chem.*, 23 (3), 583–593.

[42] Absar, N., Kalam, T.D.A., Raza, M.Q., Ashok, M., and Islam, R., 2024, Redox conditions of Early Cambrian Ocean as deciphered from multi-proxy geochemical and isotopic studies of Proto-Tethys carbonaceous sediments from Outer Lesser Himalaya, India, *J. Earth Syst. Sci.*, 133 (1), 26.

[43] Kabir, F., Bhuiyan, M.M.H., Manir, M.S., Rahaman, M.S., Khan, M.A., and Ikegami, T., 2019, Development of dye-sensitized solar cell based on combination of natural dyes extracted from Malabar spinach and red spinach, *Results Phys.*, 14, 102474.

[44] Kabir, F., Bhuiyan, M.M.H., Hossain, M.R., Bashar, H., Rahaman, M.S., Manir, M.S., Khan, R.A., and Ikegami, T., 2019, Effect of combination of natural dyes and post-$TiCl_4$ treatment in improving the photovoltaic performance of dye-sensitized solar cells, *C. R. Chim.*, 22 (9-10), 659–666.

[45] Tractz, G., Viomar, A., Dias, B., de Lima, C.A., Banczek, E.P., da Cunha, M.T., Antunes, S.R.M., and Rodrigues, P.R.P., 2019, Recombination study of dye sensitized solar cells with natural extracts, *J. Braz. Chem. Soc.*, 30 (2), 371–378.

[46] Zhou, P., Lin, B., Chen, R., An, Z., Chen, X., An, Q., and Chen, P., 2021, Effect of extending the conjugation of dye molecules on the efficiency and stability of dye-sensitized solar cells, *ACS Omega*, 6 (44), 30069–30077.

[47] Cahya, E.C., Rusliani, P.F., Suhendi, E., and Yuliarto, B., 2024, Performance of dye-sensitized solar cells with mixed three natural pigments and reduced graphene oxide as a counter electrode, *Results Opt.*, 14, 100592.